

Intravenously Injected Pluripotent Stem Cell-derived Cells Form Fetomaternal Vasculature and Prevent Miscarriage in Mouse

Cell Transplantation
Volume 29: 1–16
© The Author(s) 2020
Article reuse guidelines:
sagepub.com/journals-permissions
DOI: 10.1177/0963689720970456
journals.sagepub.com/home/ct


Atsushi Daimon^{1,2,*} , Hirofumi Morihara^{2,*}, Kiichiro Tomoda^{2,3,4,*} ,
Natsuko Morita^{1,2}, Yoshinori Koishi⁵, Kazuyoshi Kanki¹, Masahide Ohmichi¹,
and Michio Asahi²

Abstract

Miscarriage is the most common complication of pregnancy, and about 1% of pregnant women suffer a recurrence. Using a widely used mouse miscarriage model, we previously showed that intravenous injection of bone marrow (BM)-derived endothelial progenitor cells (EPCs) may prevent miscarriage. However, preparing enough BM-derived EPCs to treat a patient might be problematic. Here, we demonstrated the generation of mouse pluripotent stem cells (PSCs), propagation of sufficient PSC-derived cells with endothelial potential (PSC-EPs), and intravenous injection of the PSC-EPs into the mouse miscarriage model. We found that the injection prevented miscarriage. Three-dimensional reconstruction images of the decidua after tissue cleaning revealed robust fetomaternal neovascularization induced by the PSC-EP injection. Additionally, the injected PSC-EPs directly formed spiral arteries. These findings suggest that intravenous injection of PSC-EPs could become a promising remedy for recurrent miscarriage.

Keywords

embryonic stem cells, endothelial progenitor cells, cellular therapy, induced pluripotent stem cells, stem cell therapy

Introduction

Miscarriage is the most common complication of pregnancy, and about 15% of pregnant women experience a miscarriage¹. Women who experience three or more consecutive miscarriages before the 20th week of pregnancy are rare, but about 1% of pregnant women suffer a recurrence. Recurrent miscarriage can arise from uterine malformation, hormonal imbalance, thrombophilia, aberrant immune responses, or chromosomal abnormalities in embryos, but the cause is unknown in 40% to 50% of cases². Although aspirin and heparin improve pregnancy outcomes in women with the antiphospholipid syndrome with recurrent fetal losses³, no effective treatment exists for the many other patients with recurrent miscarriage. Because it is so emotionally traumatic, there is an urgent need to identify the causes and develop effective treatments.

DBA/2-mated CBA/J female mouse is a well-studied model of immunologically mediated or modulated pregnancy loss^{4–7} and has features similar to recurrent miscarriage in humans⁸. These mice exhibit a higher fetal

resorption rate than control BALB/c-mated CBA/J female mice⁹. Additionally, DBA/2-mated CBA/J pregnant mice resemble patients with preeclampsia in terms of significant fetal growth restriction of surviving fetuses, proteinuria, and elevated levels of soluble VEGF receptor 1 (sFlt1)^{10,11}.

¹ Department of Obstetrics and Gynecology, Osaka Medical College, Takatsuki, Japan

² Department of Pharmacology, Osaka Medical College, Takatsuki, Japan

³ Department of Life Science Frontiers, Center for iPS Cell Research and Application, Kyoto University, Japan

⁴ Gladstone Institute of Cardiovascular Disease, San Francisco, CA, USA

⁵ Division of Research Animal Laboratory and Translational Medicine, Research and Development Center, Takatsuki, Osaka, Japan

* These authors contributed equally to this article

Submitted: May 13, 2020. Revised: September 26, 2020. Accepted: October 13, 2020.

Corresponding Authors:

Kiichiro Tomoda and Michio Asahi, Department of Pharmacology, Osaka Medical College, 2-7 Daigakumachi Takatsuki, Osaka 569-8686, Japan.
Emails: pha050@osaka-med.ac.jp; masahi@osaka-med.ac.jp



Creative Commons Non Commercial CC BY-NC: This article is distributed under the terms of the Creative Commons Attribution-NonCommercial 4.0 License (<https://creativecommons.org/licenses/by-nc/4.0/>) which permits non-commercial use, reproduction and distribution of the work without further permission provided the original work is attributed as specified on the SAGE and Open Access pages (<https://us.sagepub.com/en-us/nam/open-access-at-sage>).

The DBA/2-mated CBA/J model and other animal models have provided insights into detailed mechanisms for pregnancy loss. Immunoreactions triggered by DBA/2 seminal plasma antigens, conjunctions with innate immune responses, in CBA/J female mice recruit and activate neutrophils in the decidua, which ultimately cause fetal death¹². Additionally, the immunoreactions abnormally activate natural killer (NK) cells in the decidua¹³. NK cells in the decidua induce the apoptosis of trophoblast giant cells (TGCs)¹⁴ migrating from an embryo into decidua during the early post-implantation period¹⁵. In a healthy pregnancy, the TGCs affect spiral arteries to remodel, ensuring enough blood supply to fetuses to develop¹⁵. Thus, the elimination of the TGCs by the NK cells may lead to insufficient blood supply, resulting in a fetal loss in DBA/2-mated CBA/J female mice, as well as neutrophils do^{6,8}. In contrast, increased sFlt1 may be a leading cause of the preeclampsia phenotypes, but not a fetal loss in mouse models^{16,17}.

The DBA/2-mated CBA/J model has also been useful for exploring effective treatments for recurrent miscarriage. With the model, several groups invented treatments, such as statins⁹, thrombomodulin¹⁸, or the complement component 3 (C3) inhibitor¹¹, to protect the pregnancy. Our group has shown that intravenous (IV) injection of bone marrow (BM)-derived endothelial progenitor cells (EPCs) reduced the fetal resorption rate in the same mouse model¹⁹. Thus, IV injection of BM- or peripheral blood (PB)-derived EPCs may be an effective treatment for recurrent miscarriage patients. However, the numbers of EPCs obtained from BM or PB may not be practical for treating patients. For instance, in our previous study, BM-derived EPCs collected from two to three mice were required to treat one female mouse. This problem may make it challenging to translate the findings into clinical practice.

We hypothesized that pluripotent stem cells (PSCs) (e.g., embryonic stem cells [ESCs] and induced pluripotent stem cells [iPSCs]) would be an attractive source for enough EPCs to treat patients with recurrent miscarriage. Here, we first established mouse ESC lines from preimplantation blastocysts of CBA/J-mated female CBA/J mice. By differentiating the established ESCs, we prepared cells with endothelial potential and treated DBA/2-mated female CBA/J mice with the differentiated cells. We call these cells PSC-derived cells with endothelial potential (PSC-EPs). This treatment reduced the fetal resorption rate in the model mice. Surprisingly, the injected PSC-EPs robustly promoted fetomaternal neovascularization by directly forming spiral arteries, not by substantially affecting humoral factors.

Materials and Methods

All animal procedures were performed in compliance with the guidelines of the Osaka Medical College Animal Care and Use Committee (No. 2019-084).

Derivation of ESCs from CBA/J Strain

ESCs were derived from preimplantation blastocysts of CBA/J-mated CBA/J female mice by applying the reported ESC propagation method²⁰ with slight modifications. Briefly, the embryos were flushed out from the decidua of a pregnant CBA/J mouse at 3.5 days post-coitum. The collected embryos were cultured overnight in a 35-mm dish with KSOM medium at 37°C in 5% CO₂ to obtain the blastocyst-stage embryos. The next day, embryos that normally developed to the blastocyst stage were selected. Each of the selected embryos was put on an MEF feeder cell-coated well of a 96-well plate in serum-free ESC culture medium (NDiff227, Takara Biochemicals, Japan) supplemented with leukemia inhibitory factor (10⁶ u/ml; Wako, Japan) and two kinase chemical inhibitors (PD0325901, 1 μM; ReproCELL, Japan; CHIR99021, 3 μM; Wako, Japan). After a few days, the blastocysts were attached on the well, and cells grew from them. The expanded cells were passaged by dissociation with Accutase (Funakoshi, Japan). We define this passage event as the passage (p)1. Until p3, the expanded cells were maintained on MEF feeders with the same ESC culture medium. At p4, the cells were passaged on a laminin (iMatrix-511 silk, 1.25 μg/ml; Takara Biochemicals, Japan)-coated well and, after this, maintained under the feeder-free condition with the same ESC culture medium.

Generation of Green Fluorescent Protein–Labeled ESCs

To label ESCs with green fluorescent protein (GFP), a vector containing a GFP-expressing cassette was transfected into the cells using Lipofectamine 2000 (Thermo Fisher, MA), according to the manufacturer's instruction. Briefly, the day before transfection, ESCs were seeded in six-well plates (70% to 90% confluent per well) using an ESC culture medium. Lipofectamine/DNA was prepared in Opti-Mem Medium (Thermo Fisher, MA) by mixing 2.5 μg of the vector with 10 μl of Lipofectamine 2000 transfection reagent for a well of a six-well plate. Before mixing, the vector was diluted with 150 μl of Opti-Mem Medium and Lipofectamine 2000 with 150 μl of Opti-Mem Medium. The Lipofectamine/DNA mixture was left for 5 min at room temperature to form a complex before adding it to the cells. The DNA–lipid complex was added with ESC culture medium, and the ESCs were cultured for 1 to 3 days at 37°C. The vector contains a puromycin-resistant gene expression cassette. Therefore, transfectants were selected with 1 μg/ml puromycin for 2 days. GFP expression was confirmed by fluorescent microscopic inspection.

Isolation of Total RNA

Total RNA was purified from the ESCs, differentiated ESCs, or placental tissues using the RNazol RT (Cosmo Bio, Japan), according to the manufacturer's instructions.

Absorbances of RNA at 260 and 280 nm were measured with NanoDrop ND-1000 spectrophotometer (Thermo Fisher, MA). RNA samples that exhibited optical density (OD) 260/OD 280 ratios greater than 1.80 were used for further processing, and all RNA samples used met this purity requirement.

Real-Time Polymerase Chain Reaction

Total RNA (400 ng/sample) was reverse-transcribed to generate a cDNA template with PrimeScript RT reagent Kit (Takara Biochemicals, Japan), according to the manufacturer's protocol. The RT mixture was made in a 20- μ l reaction volume, and the RT was performed with Takara PCR Thermal Cycler (Takara Biochemicals, Japan) with settings as follows: 37°C for 15 min, 85°C for 5 s, and 4°C until finished. Polymerase chain reaction (PCR) was performed with Ex Taq (Takara Biochemicals, Japan) as follows: denaturation at 98°C for 1 min; 30 to 40 cycles of annealing at 58 to 60°C for 30 s; and extension at 72°C for 1 min. PCR primers and annealing cycles and temperature are summarized (Supplemental Table 1).

Nanog, *Pou5f1*, *Zfp42*, *Tall1*, *Egr4*, *Flt-1*, *Vegfa*, *Plgf*, and *Gapdh*, *Cd34* gene expressions were evaluated by quantitative PCR using pre-designed mouse *Nanog* (Mm02019550_s1), *Pou5f1* (Mm03053917_g1), *Zfp42* (Mm03053975_g1), *Tall1* (Mm01187033_m1), *Egr4* (Mm00842279_g1), *Flt-1* (Mm00438980_m1), *Vegfa* (Mm00437306_m1), *Plgf* (Mm00435613_m1), and *Gapdh* (Mm99999915_g1), *Cd34* (Mm00519283_m1), and TaqMan Gene Expression Master Mix with Step One Plus Real-Time PCR system (Thermo Fisher, MA). Samples were assayed in triplicates in a 10- μ l reaction volume with the following thermal cycler settings: 1 cycle of 50°C for 2 min and 95°C for 20 s, followed by 40 cycles of 95°C for 1 s and 60°C for 20 s. *Gapdh* was used to normalize Ct values from each of the other probes. PCR reactions without cDNA templates served as negative controls in each experiment.

Differentiation of ESCs by the Embryoid Body Formation

ESC colonies were entirely dissociated into single cells. The dissociated cells were seeded on a 10-cm dish for suspension culture (1.0×10^6 cells per dish) in Dulbecco's modified Eagle medium basic (DMEM basic, Thermo Fisher, MA) supplemented with 20% fetal bovine serum (Thermo Fisher, MA). The seeded cells were cultured for 7 days to allow for embryoid body (EB) formation. The EBs were then transferred to gelatin-coated six-well plates and cultured in the same medium for 10 days. After 10 days, total RNA was extracted from the cells growing from the EBs, using the RNazol RT (Cosmo Bio Co, Japan) according to the manufacturer's instructions.

Differentiation of ESCs into the Endothelial Cell Lineage

ESCs were differentiated into the endothelial cell lineages using the endothelial differentiation protocol developed for human PSCs²¹ with some modification. Our differentiation protocol consists of two phases. First, ESCs were differentiated into epistemic cell (EpiSC)-like cells²² (phase I). Second, the EpiSC-like cells were differentiated into the endothelial cell lineages²¹ (phase II). At phase I, ESC colonies were entirely dissociated into single cells and seeded on a well of a six-well plate coated with Fibronectin (0.1%, Sigma) in ESC-cultured medium. One day after the culture, the medium was changed to NDiff227 medium supplemented with Activin A (20 ng/ml; Wako, Japan), basic FGF (12 ng/ml; Wako, Japan), and Rho kinase inhibitor (Y-27632, 10 μ M). The cells were continuously cultured for 2 days (phase I). Then, the cells were cultured in DMEM with B27 without insulin (50 \times ; Thermo Fisher, MA) supplemented with GSK 3 α - β inhibitor (CHIR-99021, 10 μ M) for 2 days. Finally, they were cultured in endothelial cell growth medium (EBM2; Lonza, Basel, Swiss) for 3 days (phase II).

Immunofluorescence Staining

Cells were stained with phycoerythrin-conjugated monoclonal antibodies against cell-surface markers, CD34 (1:100; eBioscience, CA), CD31 (PECAM-1) (1:100; eBioscience, CA), CD45 (1:100; eBioscience, CA), and VE-cadherin (1:100; Santa Cruz Biotechnologies, TX), to characterize the differentiated cell phenotypes. The differentiated cells were fixed with 4% paraformaldehyde (PFA) (Nacalai Tesque, Japan) for 10 min, permeabilized with Triton X-100 (0.1%) in phosphate-buffered saline (PBS) for 10 min, and then incubated with bovine serum albumin (BSA) (5%) for 10 min, followed by overnight incubation with the primary antibodies in 5% BSA in PBS at 4°C. The next day, the cells were washed with PBS twice, and the nuclei were stained with 4',6-diamidino-2-phenylindole. Then, the staining samples were inspected with a fluorescent microscope.

In Vitro Tube Formation Assay

In day 4 of endothelial differentiation culture, 2.5×10^5 differentiated ESCs were seeded on a well of a 24-well plate precoated with growth factor-reduced Matrigel (Corning, NY) and cultured in the endothelial medium for 24 h at 37°C. Images were taken with a light microscope.

Incorporation of Acetylated Low-Density Lipoprotein

ESCs (negative control) and differentiated ESCs in day 4 of endothelial differentiation culture were incubated with 1,10-dioctadecyl-1-3,3,30,30-tetramethylindocarbocyanine-perchlorate-acetylated-low density lipoprotein (10 μ g/ml; Alfa Aesar, MA) for 4 h at 37°C. After the incubation, the

cells were washed with PBS and imaged by fluorescent microscopy.

Animal Experiments

Inbred CBA/J and DBA/2 mice from The Charles River Laboratory were used. Virgin female CBA/J mice (10 to 14 weeks old) were mated male DBA/2 mice (8 to 14 weeks old). Female mice were inspected daily for vaginal plugs, and the presence of a vaginal plug was defined as day 0.5 of pregnancy. Differentiated ESCs on day 4 of endothelial differentiation culture (5×10^5 in 150 μ l of PBS/mouse) or PBS alone (control group) were injected into pregnant female mice via a tail vein on day 7.5 of pregnancy.

On day 10.5 of pregnancy, 1 ml of fluorescein isothiocyanate (FITC)-conjugated dextran (2 mg/ml in PBS, averaged molecular weight 150,000, Merk, MO) was intravenously injected into pregnant mice. The injected mice were sacrificed 15 min after the injection. Livers and placentae were collected from the mice. And then, fluorescence signals from the FITC-dextran were examined by a fluorescent microscope, as described below.

On day 14.5 of pregnancy, pregnant females were euthanized, and the decidua, including placenta and embryo, and blood were collected. The fetal resorption rate was calculated as described in the figure legends with Excel or JMP software, and the collected samples were used for the downstream analyses.

CUBIC Protocol for Whole-Organ Clearing

The tissue cleaning method was used in this study²³. Collected whole deciduae were postfixed in 4% PFA (Nacal Tesque, Japan) in PBS at 4°C for 24 h. The deciduae were washed with PBS for more than 2 h three times with gentle shaking to remove PFA just before clearing. The fixed whole deciduae were immersed in 50% CUBIC-L+ (1:1 mixture of water and CUBIC-L+) for 24 h and further soaked in CUBIC-L with gentle shaking at 37°C for 5 days. The deciduae were washed with PBS at room temperature for more than 2 h three times with gentle shaking. They were then subjected to immunostaining with the 1:100 diluted antibodies (Alexa Fluor 647 Rat Anti-Mouse CD31; BioLegend, CA) in a staining buffer containing 5% BSA and 0.5% Triton X-100 for 3 days at 4°C with shaking. The stained samples were washed with PBS three times at room temperature with shaking. Then they were immersed in 50% CUBIC-R (1:1 mixture of water and CUBIC-R) for 24 h and further immersed in CUBIC-R with gentle shaking at 37°C for 3 days.

Fluorescent Microscope and Confocal Microscope

The stained *in vitro* differentiated cell images were taken using a fluorescence microscope (BZ-X710, Keyence, Japan). The images for tiling Z-stacks of the deciduae, including fetuses and placentae, were acquired with a

confocal microscope (TSC-SP8, Leica), according to the manufacturer's instructions. After the acquisition, the decidua was reconstructed with the images using microscope software and Photoshop. We observed very faint signals from blood vessel-like structures in nonstained and non-cell-injected control deciduae, suggesting autofluorescence signals. However, they were too weak to affect the conclusion.

Quantifications of CD31+ Blood Numbers, Diameters, and Densities

After obtaining images, the numbers of CD31+ blood vessels in the images were manually counted. The diameter of the CD31+ stained blood vessels in the images was quantified by the WinROOF digital image analyzer (Mitani, Japan) by manually drawing a perpendicular line to the blood vessel analyzed. The areas of the CD31+ stained blood vessels were also measured using the image analyzer, and the percentages of the CD31+ blood vessel densities were calculated by dividing the total of the CD31+ areas by the entire cross-sectional area of the placenta specimen.

Enzyme-linked Immunosorbent Assays

Blood samples were collected from the pregnant females on day 14.5 of pregnancy and allowed to clot for 2 h at room temperature before centrifuging for 20 min at 2,000 \times g. After centrifugation, serum was collected and assayed immediately or aliquoted and stored at -30°C until use. Seventy-five microliters of serum was used to measure concentrations of secreted sFlt1 with commercially available enzyme-linked immunosorbent assay (ELISA) kits, according to the manufacturer's instructions (R&D Systems, MN). After the ELISA reaction, optical densities were measured at 450 nm with a microplate ELISA reader (SPECTRA MAX 190; Molecular Devices, CA). The average of the duplicate readings for each standard, control, and individual samples was used for the analysis.

Results

Establishing and Characterizing CBA/J-Derived ESC Lines

We hypothesized that PSC-derived EPCs could be substituted for the BM-derived cells to prevent miscarriage in model mice. Since autologous transplantation of the PSC-derived differentiated cells does not cause severe immunoreactions in hosts²⁴, CBA/J-derived PSCs, either ESCs or iPSCs, are the best source for EPCs to test the hypothesis. However, CBA/J-derived PSCs have never been reported. Further, it may be easier to generate high-quality mouse ESCs than high-quality mouse iPSCs, although their functionality is not distinguished. These situations prompted us to establish ESC lines from embryos of CBA/J-mated CBA/J females. By applying the reported mouse ESC

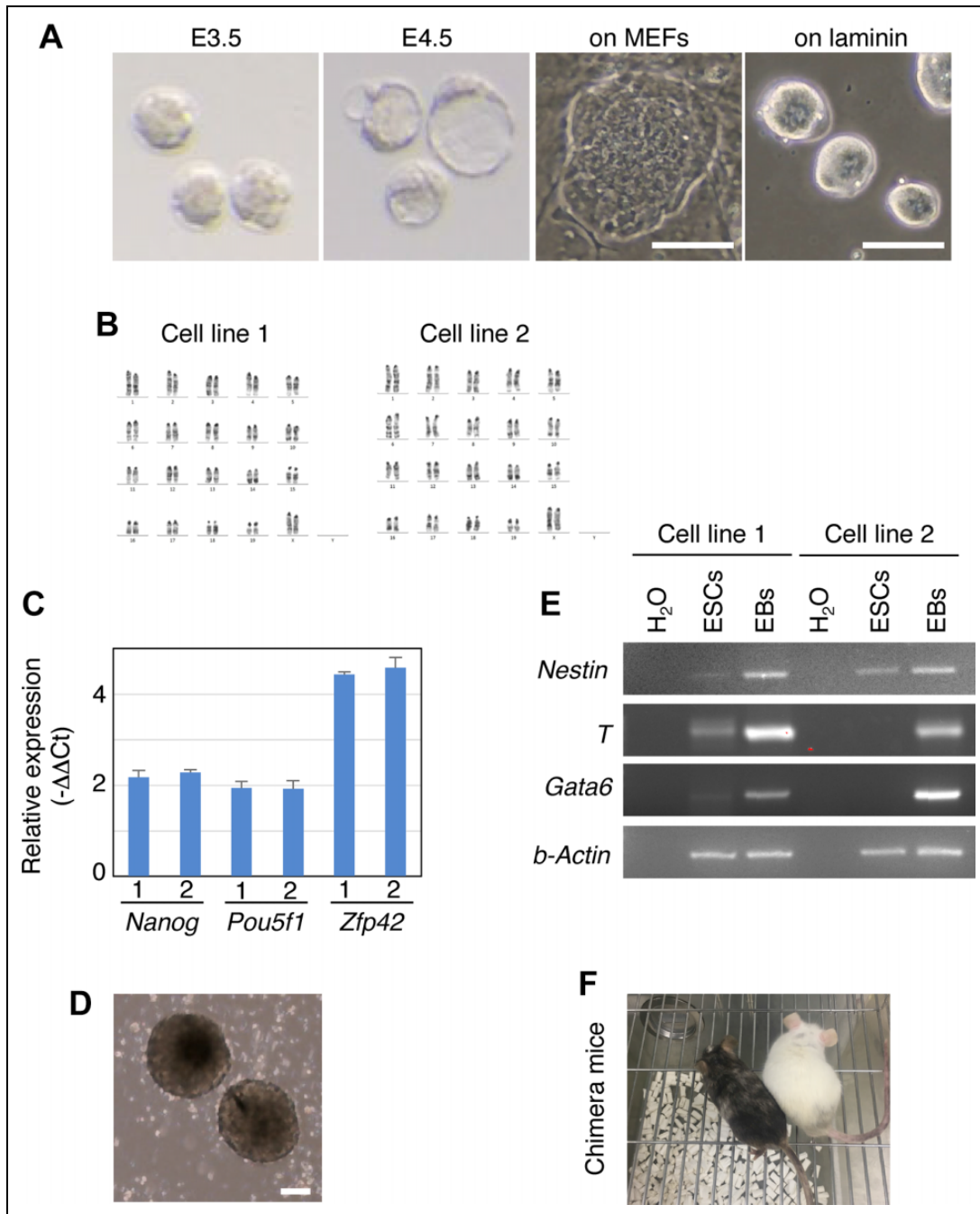


Figure 1. Establishment and characterization of CBA/J-derived ESC lines. (A) Images for preimplantation embryos and colonies of cells established from the embryos. Size bar = 100 μ m. (B) Karyotype of two cell lines by G banding. (C) Expression of pluripotency marker genes. Reverse transcription and quantitative polymerase chain reaction was performed using RNA extracted from the cell lines showing a normal karyotype in (B). Probes are indicated. Ct values obtained with the indicated probes were normalized to those with *Gapdh* (ΔCt) and then normalized with ΔCt s from authentic ESCs E14 ($\Delta\Delta Ct$ s). The negative values of the $\Delta\Delta Ct$ s are shown in the graph. Mean \pm SD. $n = 3$. (D, E) The ability of the cell lines to differentiate *in vitro* by EB formation. Image of EBs (D). Real-time polymerase chain reaction was performed with RNA from attached EB-derived cells and revealed that ectoderm (*Nestin*), mesoderm (*T*), and endoderm (*Gata6*) marker genes were induced, compared with those in ESCs. H₂O samples were obtained from PCR with no RNA and served as negative controls. Size bar = 100 μ m. (F) Photo of newborn chimeras after blastocyst injection of the CBA/J-derived ESCs. The brown coat color of the mouse indicates the high contribution of the ESCs to mouse development. EB: embryoid body; ESC: embryonic stem cell.

propagation method²⁰ with slight modifications, five cell lines were established from preimplantation blastocysts in a culture medium containing LIF and two chemical kinase inhibitors²⁵ on laminin-coated plates (LIF+2i condition) (Fig. 1A). They exhibited dome-shaped colony morphologies that resembled colonies of authentic ESCs derived from 129 mouse strains in these culture conditions. G banding of all cell lines identified two with a normal karyotype (Fig. 1B and Supplemental Fig. 1A). Thus, we focused on these two cell lines with normal karyotypes.

PSCs have two distinct features: the ability to self-renew infinitely *in vitro*, and the ability to differentiate into any type of cells in the three germ layers. We next examined if the established cell lines exhibit the features of PSCs. They proliferated well with a doubling time of about 24 h in LIF+2i (Supplemental Fig. 1B). During a 5-month culture, their proliferation rate and colony morphology did not change.

To examine the expression of pluripotency marker genes, RNA was collected from the cell lines and subjected to reverse transcription and quantitative polymerase chain reaction (RT-qPCR) of the extracted RNA. This analysis revealed that the pluripotent marker genes tested were highly expressed in the established cell lines, comparable to those in the 129 derived ESCs (Fig. 1C).

Next, the ability of the cell lines to differentiate *in vitro* was tested by EB formation. ESCs were detached from a plate and cultured in suspension in the differentiation medium. After 8 days in culture, the cells formed EBs (Fig. 1D). When the EBs were put on a gelatin-coated plate, they were attached to the plate. The attached EBs were further cultured on the plate for 10 days in the differentiation medium. After the culture, RNA was collected from the attached cells. Real-time polymerase chain reaction analysis with the extracted RNA revealed that ectoderm (*Nestin*), mesoderm (*T*), and endoderm (*Gata6*) marker genes were more highly expressed in the attached cells than in undifferentiated ESCs (Fig. 1E). These results suggest that the cell line can be differentiated into the three germ layers. Additionally, the ESCs could highly contribute to mouse development *in vivo* by blastocyst injection (Fig. 1F). Collectively, the cell lines exhibited the features of PSCs, and thus, we concluded that they were bona fide CBA/J-derived ESCs.

Differentiation of the ESCs Into the Endothelial Lineage

To propagate enough PSC-derived EPCs for transplantation, we used a differentiation protocol developed for human PSCs²¹. This simple protocol produces high-quality human PSC-derived endothelial cells²¹. With some modifications to the protocol (Fig. 2A), we differentiated the ESCs to cells that exhibited features of endothelial cells.

To monitor the differentiation, we obtained RNA from undifferentiated ESCs and the differentiating cells each day beginning at day 1 of the differentiation and examined

pluripotent markers (*Nanog*, *Zfp42*, and *Pou5f1*) by RT-qPCR (Fig. 2B). These experiments revealed that *Nanog* and *Zfp42* were immediately downregulated (about 10-fold) at day 1, relative to the undifferentiated ESCs, and the low levels were maintained till day 6. The other pluripotent marker, *Pou5f1*, was gradually downregulated and was at its lowest level (52-fold less than undifferentiated ESCs) on day 6 (Fig. 2B). These results suggest that the ESCs begin to exit from the pluripotent state on day 1.

Next, we determined when the differentiated cells entered into the endothelial lineage by examining the mRNA expression of vascular endothelial markers (*Tall* and *Egr4*). *Tall* was upregulated from day 2, and the high level was maintained until day 4 (Fig. 2C), and *Egr4* was maintained at a low level but was sharply induced on day 3 (Fig. 2C). Since these genes were induced at an endothelial precursor stage²⁶, we concluded that the differentiated cells were in an endothelial lineage on day 4. Therefore, we further characterized cells on day 4 of the differentiation.

We looked for the expression of additional markers by staining differentiated cells with antibodies against CD31 (PECAM-1), VE-cadherin or CD34, cell-surface antigens for endothelial cells. We found that these markers were positive in differentiated cells (Fig. 2D and Supplemental Fig. 1C). Flow cytometric analyses revealed $12.75\% \pm 1.2\%$ of the cells analyzed were CD31+ in the differentiated culture but could not detect CD34+ cells (Supplemental Fig. 1D). To confirm the CD34 expression, we examined CD34 mRNA and found that it was indeed upregulated in the differentiated cells, compared with ESCs (Supplemental Fig. 1E). Thus, our enzyme treatment to prepare the flow samples may affect the cell-surface marker expressions (e.g., Ref²⁷). In contrast, the culture was completely negative for CD45, a marker for the blood lineages, both with microscopic and flow cytometric analyses (Fig. 2D and Supplemental Fig. 1D).

Endothelial cells can incorporate acetylated low-density lipoproteins (Ac-LDLs)²¹. When ESCs were treated with fluorescence-conjugated Ac-LDLs, ESCs did not take them up and were entirely negative for the fluorescence (Fig. 2E, top). In contrast, almost all the differentiated cells became weakly positive, and some showed strong fluorescence signals (Fig. 2E, bottom). These data suggest that most differentiated cells incorporated Ac-LDLs with a substantial difference in the amount of uptake.

Finally, the functionality of the differentiated cells as endothelial cells was evaluated *in vitro* by the tube formation assay²¹. Differentiated cells on day 4 were detached from a plate and seeded on a Matrigel-coated plate. Within 24 h, the seeded cells formed vascular network-like structures, and few cells were attached on the plate without forming the structures (Fig. 2F). These results indicated that most day 4 differentiated cells robustly exhibit the endothelial potential despite the low percentage of CD31+ cells. We call these cells PSC-EPs.

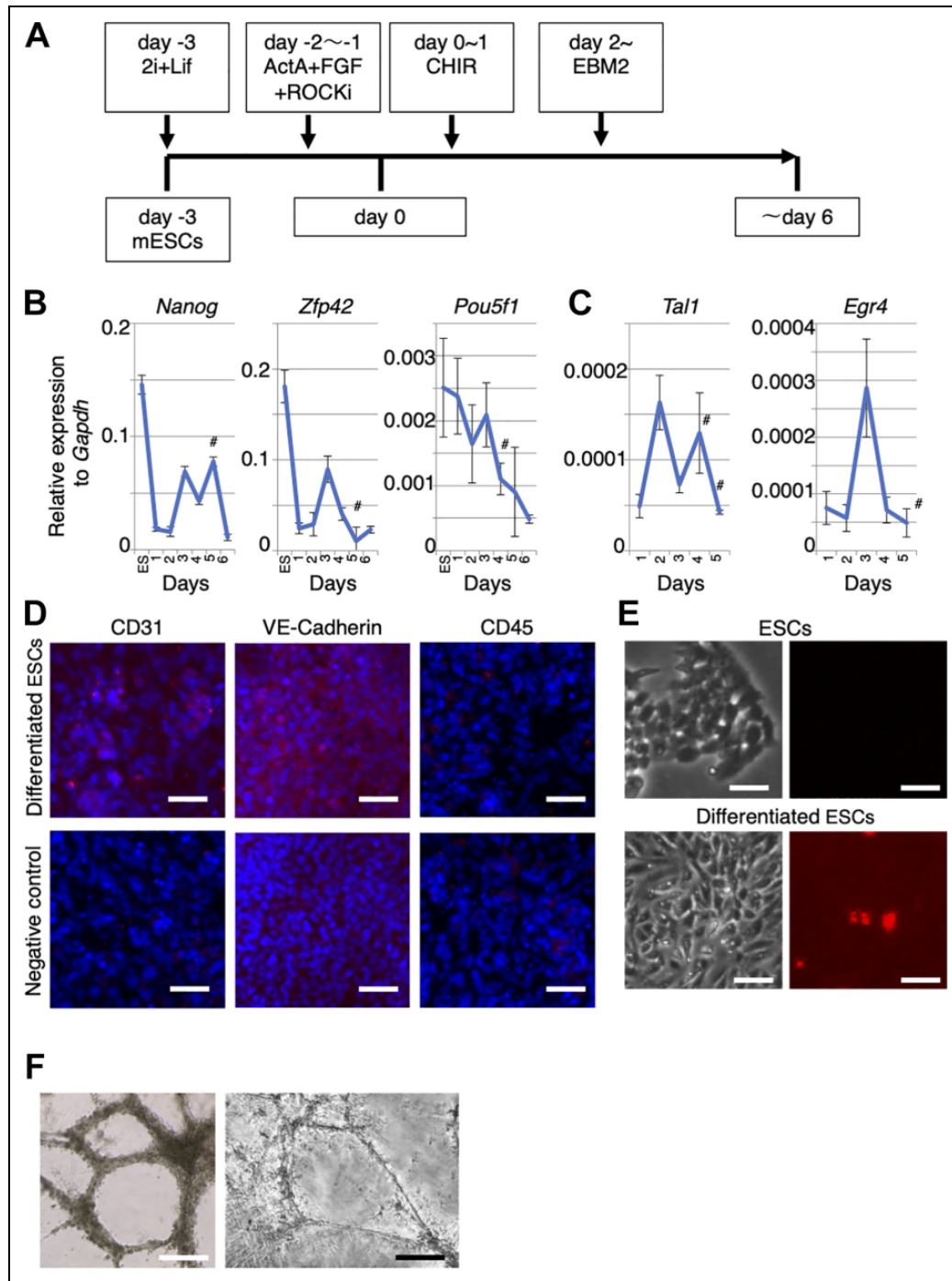


Figure 2. Differentiation of ESCs into the endothelial lineage. (A) Endothelial differentiation protocol. (B, C) Changes in the expression of pluripotent markers (*Nanog*, *Zfp42*, and *Pou5f1*) (B) and vascular endothelial markers (*Tal1* and *Egr4*) (C) during the differentiation into endothelial lineages. Reverse transcription and quantitative polymerase chain reaction was performed using RNA extracted from cells at the indicated time points during differentiation. Probes for qPCR are indicated. Ct values obtained with the indicated probes were normalized by those with *Gapdh* (Δ Ct) to calculate the relative expression values, and the values are plotted. Mean \pm SEM. $n = 3$. # indicates the time at which one sample was undetectable. (D) Immunofluorescence staining (red) of differentiated cells using a specific antibody against CD31 (PECAM1), CD45, or VE-cadherin. DNA (blue) was stained with 4',6-diamidino-2-phenylindole. The size bar = 50 μ m. (E) Fluorescent microscopic images for Dil-Ac-LDL uptake (red). ESCs (top images) or day 4 differentiated cells (bottom) were treated with Dil-Ac-LDL for 4 h. After washing, the bright-field (left) or fluorescent (right) images were taken. Size bar = 50 μ m. The fluorescence images were taken with the same condition. (F) Bright-field microscopic images of the differentiated cells forming a tube-like structure on a Matrigel-coated plate. Size bar = 20 μ m (left) and 300 μ m (right). Two images were taken 24 h after the day 4 differentiated cells were seeded on the plate. Two different microscopes were used for taking the images to clarify the tube-like structures formed by the differentiated cells. Dil-Ac-LDL: 1,10-dioctadecyl-1-3,3,30,30-tetramethylindocarbocyanineperchlorate-acetylated-low-density lipoprotein; ESC: embryonic stem cell.

A Decrease in Number of Placentae That Exhibit Hypoperfusion by IV Injection of PSC-EPs

In several mouse models of pregnancy loss, including the DBA/2-mated CBA/J female mouse, abnormal placentation, including placental hypoperfusion, frequently occurs⁹ and seems to be a leading cause of the ultimate fetal death^{14,15}. Thus, we first determined if placental hypoperfusion occurs in our DBA/2-mated CBA/J females as reported⁹. Since fetomaternal vasculature formed by day 10.5 of pregnancy²⁸, we dissected and analyzed the pregnant females at day 10.5. Right before the dissection, fluorescent-conjugated dextran was intravenously injected into the mice to monitor blood perfusion (Fig. 3A). Intensities of fluorescence signals from the injected dextran in the placenta reflect an amount of blood reaching the placenta^{9,29} (Fig. 3B, C). We found that, in control mice, 31% of placentae analyzed (Fig. 3D), or 9 out of 29 placentae (Fig. 3E), exhibited reduced fluorescence intensity by less than 0.8 of the mean intensity.

Since PSC-EPs exhibited considerable endothelial potential (Fig. 2F), we next tested if IV injection of PSC-EPs into DBA/2-mated CBA/J females would increase blood supply and reduce the placental hypoperfusion. To this end, injection experiments were designed, based on our previous study¹⁹. Nonlabeled PSC-EPs were prepared and IV injected into DBA/2-mated CBA/J females at day 7.5 of pregnancy, and the pregnant females were euthanized at day 10.5 to evaluate the blood supply (Fig. 3A). We found that only <10% of the placentae analyzed, or 3 out of 32 placentae, exhibited lower fluorescence signals (Fig. 3D, E). As a control, we examined fluorescence signals in the livers of the mice and found that fluorescence signals in the PSC-EP-injected mice were similar to those in the PBS-injected mice. Thus, the amount of dextran injected did not differ in the two groups (Supplemental Fig. 2A). Collectively, these results suggest that some placentae of DBA/2-mated CBA/J females indeed exhibited severe hypoperfusion and that IV injection of PSC-EPs reduced the placental hypoperfusion at the early post-implantation stage significantly.

Reduction of Fetal Resorption by IV Injection of PSC-EPs

We next tested if IV injection of PSC-EPs would reduce fetal resorption rates of the DBA/2-mated CBA/J females (Fig. 3). The experiments were designed similarly to those in Fig. 3, but the injected pregnant mice were analyzed at day 14.5 to evaluate fetal resorption (Fig. 4A). At the same time, controls, PBS, or BM-derived EPCs were injected separately into pregnant females (Fig. 4A).

By day 14.5 of pregnancy, about 25% of the DBA/2-mated CBA/J miscarry^{4,6,9,10} (Fig. 4B). Indeed, PBS-injected females showed almost the same loss ($27.3\% \pm 4.17\%$) or had 33 resorbed out of 124 embryos (Fig. 4C, D). However, the PSC-EP-injected females had a significantly lower resorption rate ($7.8\% \pm 2.86\%$) than the PBS controls or

11 resorbed out of 149 (Fig. 4C, D, and Supplemental Fig. 2B). The reduction in the resorption rate by PSC-EP injection was comparable to or slightly more significant than that of the BM-derived EPC injection (Fig. 4C). Thus, PSC-EPs possess the ability to ameliorate miscarriage till day 14.5 of pregnancy in the mouse model.

Robust Establishment of Fetomaternal Vasculature by PSC-EPs

During early pregnancy, substantial growth and remodeling of spiral arteries, which are triggered by TGCs migrating from embryos, occur to supply enough fetomaternal blood flow that is required for normal placentation and embryonic development. Failure of the remodeling is thought to cause pregnancy complications, such as preeclampsia in mice and humans^{14,15,30}. Our previous study showed that IV injection of BM-derived EPCs enhances placental vascularization, but detailed degree and mechanisms of the vascularization remain obscure¹⁹.

Here, we investigated the establishment of fetomaternal vasculature in PBS- and PSC-EP-injected females. Pregnant females at day 14.5 were euthanized, and deciduae, including placentae and embryos, were collected and analyzed. To obtain information on the three-dimensional architecture of the vasculature in the decidua, we utilized the tissue-cleaning technique²³ and extensive tiling of Z-stack images of the decidua captured by confocal microscopy. We found that the deciduae in the PSC-EP-injected females contained more spiral arteries, judged by morphology and CD31 staining, than those in the PBS controls (Fig. 5A and Supplemental movies 1 and 2). Additionally, the diameter and density of the spiral arteries in the PSC-EP-injected females were more significant than those in the PBS controls (Fig. 5B). Therefore, IV injection of the PSC-EPs induces the development of spiral arteries.

PSC-EPs efficiently formed vascular-like structures *in vitro* (Fig. 2F). Thus, we determined if the injected PSC-EPs directly formed the spiral arteries *in vivo* using cells labeled with a GFP (Supplemental Fig. 2C). This analysis revealed that the spiral arteries in GFP-labeled PSC-EP-injected females, but not PBS controls, were strongly GFP positive (Fig. 5C). Collectively, these results indicate that the injected PSC-EPs migrated to the implantation site, colonized there, and were subsequently incorporated into the spiral arteries. This incorporation may make it possible to establish the fetomaternal vasculature that supplies blood sufficient to maintain placentation and embryonic development in DBA/2-mated CBA/J females.

No Substantial Effects of PSC-EP Injection on the Angiogenic Factor Balance in DBA/2-Mated CBA/J Females

DBA/2-mated CBA/J females have the abnormal expression of angiogenic (Vegf α and Plgf)¹⁰ and anti-angiogenic (sFlt1)

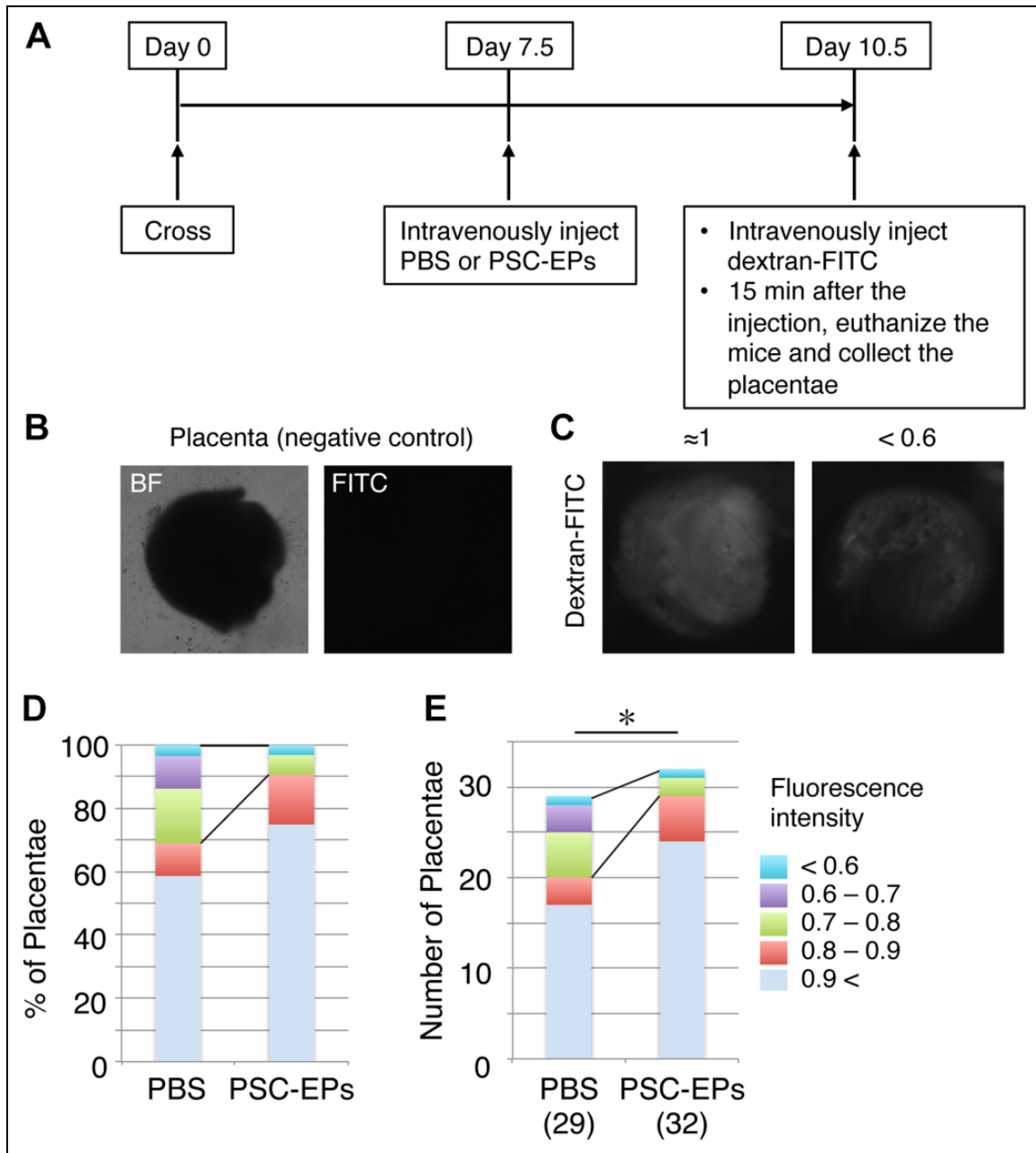


Figure 3. A decrease in number of placentae that exhibit hypoperfusion by intravenous injection of PSC-EPs. (A) The experimental design. (B, C) Images of placentae without (B) or with (C) the injection of fluorescence-conjugated dextran. The fluorescent image in (B) serves as a negative control for (C). (C) shows the examples of the fluorescent signals in placentae; the left shows the fluorescence signals whose intensity is close to the mean intensity among the placentae analyzed, and the right shows a decrease in the fluorescence intensity by <0.6 of the mean. (D, E) Classification of the placentae by fluorescence signals from the injected dextran. The fluorescence intensities used for the classification and numbers of the placentae analyzed are shown in (E). $n = 29$ (PBS) and 32 (PSC-EPs) placentae. Chi-squared test for the placentae that exhibited reduced fluorescence intensities by <0.8 of the mean in each group. $*P < 0.05$. PBS: phosphate-buffered saline; PSC-EPs: PSC-derived cells with endothelial potential.

factors¹⁸, and exhibit angiogenic factor imbalance. Further, transplanted BM- or PB-derived EPCs, or mesenchymal stem cells (MSCs) frequently release humoral factors that may modulate angiogenesis.

We determined if IV injection of PSC-EPs affects angiogenic or anti-angiogenic humoral factors in DBA/2-mated CBA/J females. RNA was collected from individual healthy

and aborted deciduae, including placentae, from DBA/2-mated CBA/J females at day 14.5 of pregnancy. The quality of RNA extracted from the healthy or aborted deciduae did not substantially differ, and RT-qPCR examined the genes in each sample. Their expressions did not significantly differ between the PSC-EP- and PBS-injected samples, except for *Plgf* (placental growth factor) (Fig. 6A-D). *Plgf* encodes the angiogenic factor

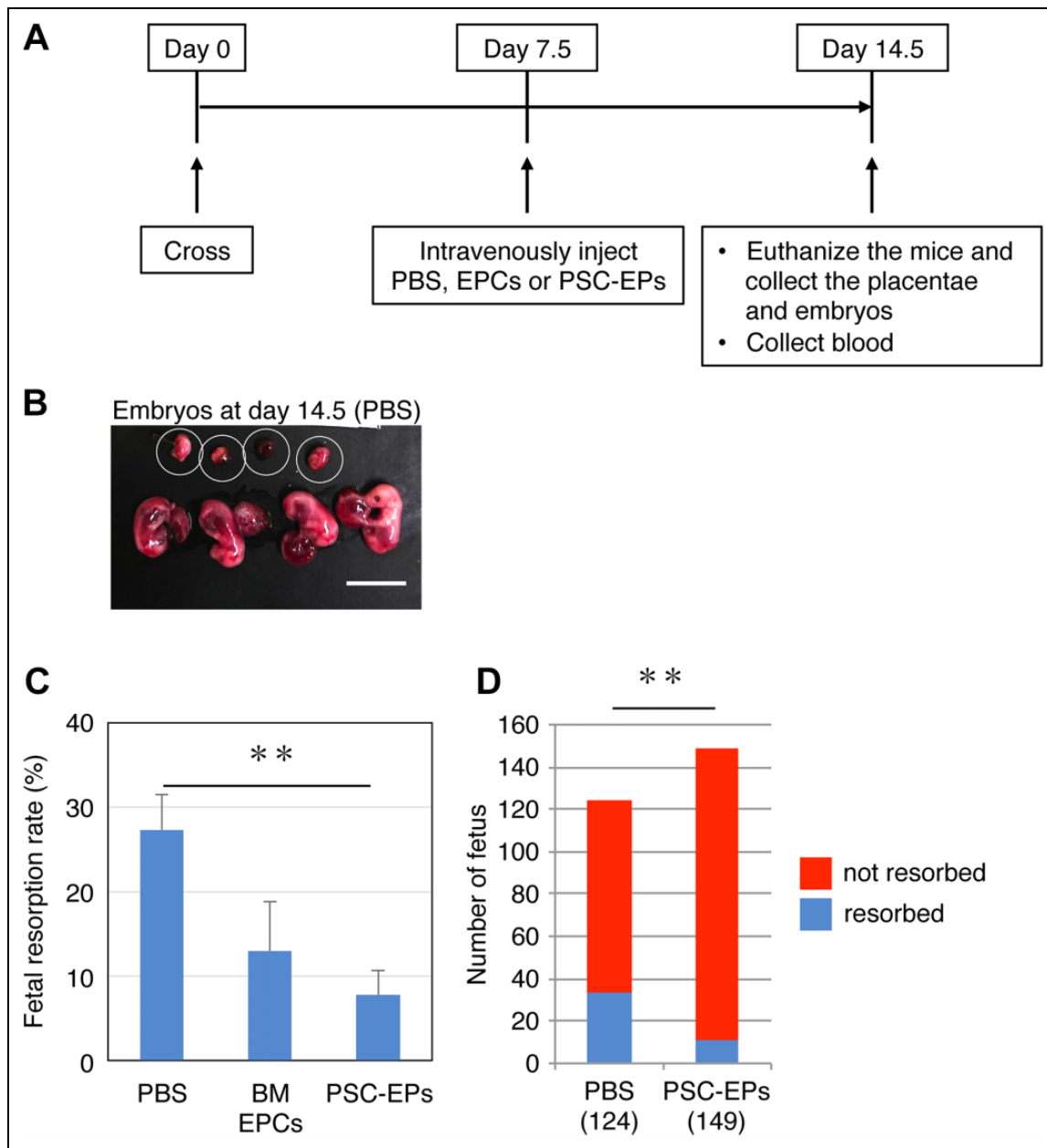


Figure 4. Reduction of fetal resorption by intravenous injection of PSC-EPs. (A) The experimental design. (B) Images of embryos, including placentae, collected from a DBA/2-mated CBA/J female mouse at day 14.5 of pregnancy. Circles in the image indicate resorptions. Size bar = 13 mm. (C) Fetal resorption rates with the indicated treatments. Rates were calculated by dividing the number of resorbed embryos with a total number of embryos in a pregnant mouse, and then the mean rate in each condition was calculated. Mean \pm SD. $n = 17$ pregnant mice (PBS), 5 (BM EPCs), and 22 (PSC-EPs). Wilcoxon rank-sum test. $**P < 0.01$. (D) Number of embryos that were resorbed or not resorbed. $n = 124$ (PBS) and 149 (PSC-EPs) embryos. Chi-squared test for the resorbed embryos in each group. $**P < 0.01$. BM: bone marrow; EPC: endothelial progenitor cell; PBS: phosphate-buffered saline; PSC-EPs: PSC-derived cells with endothelial potential.

but was lower in the PSC-EP-injected samples than the controls (Fig. 6C). We also examined the systemic sFlt1 protein levels at day 14.5 by ELISA and found no differences (Fig. 6E). Therefore, the PSC-EPs prevent a fetal loss without affecting the angiogenic factor balance at day 14.5 in the model mice. Also, the treatment effect of PSC-EPs may be independent of their ability to secrete the humoral factors. This latter finding

may differ from what was observed with BM- or PB-derived EPCs, or MSCs.

Discussion

Using newly established ESC lines, we showed here that IV injection of PSC-EPs increased blood supply to the

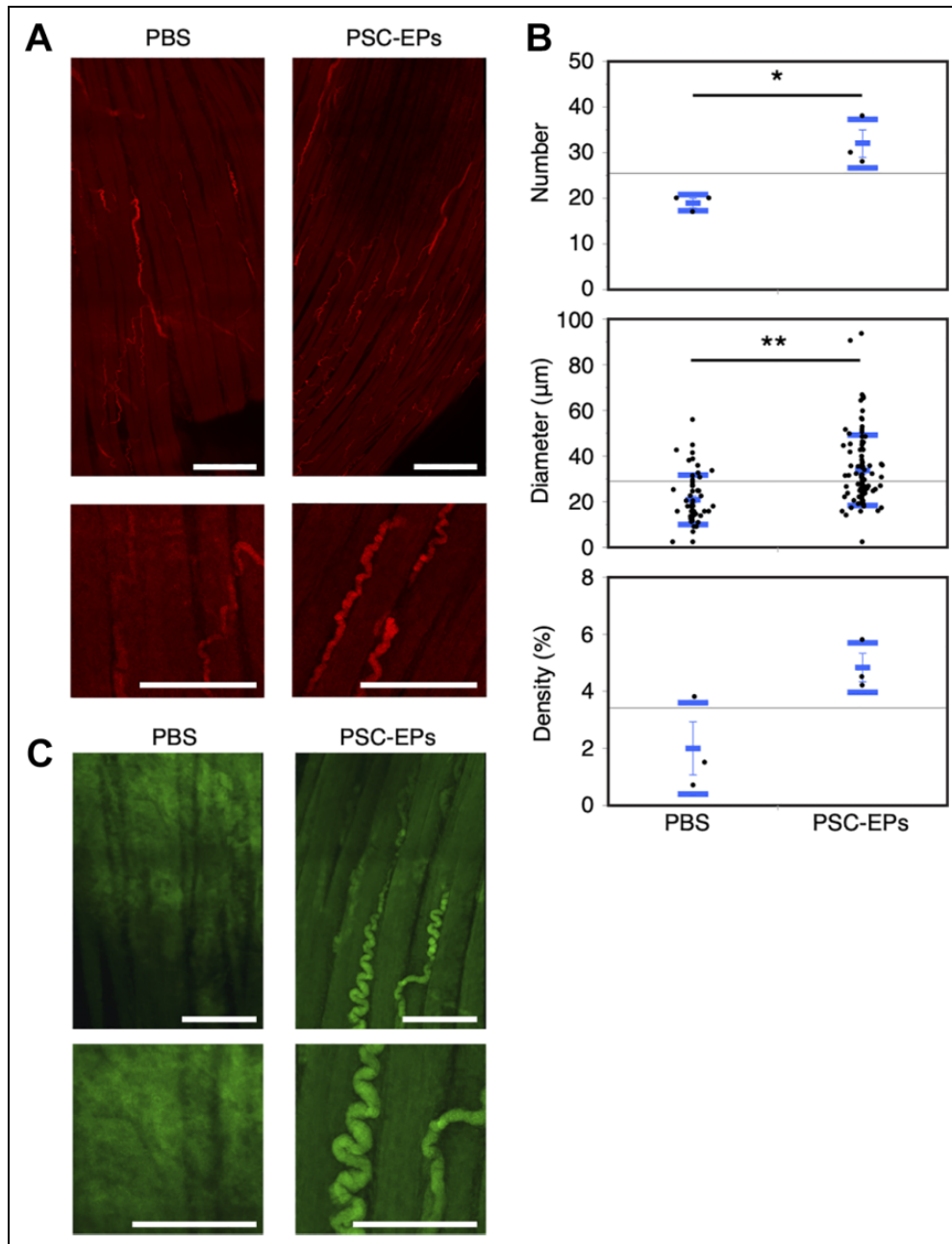


Figure 5. Robust establishment of spiral arteries by intravenous injection of PSC-EPs. (A, C) The reconstruction of the tiling Z-stack fluorescent images of the placenta collected from a PBS or PSC-EP-injected female mouse. In (A), the placenta was stained with an antibody against CD31 (red) before the imaging. In (C), PBS or PSC-EPs from GFP-labeled PSCs were intravenously injected into a DBA/2-mated CBA/J female mouse. The placenta was collected from the mouse, and GFP signals (green) in the reconstructed placenta images were captured. The top images show the entire placenta captured from an embryo. The bottom images are enlarged ones from the top. Size bar = 750 (top) and 300 μm (bottom) in (A), 300 (top) and 200 μm (bottom) in (C). (B) Number, diameter, or density of spiral arteries in placenta images. Mean (short blue bar) \pm SD (long blue bars). $n = 3$ for each group (number and density). For diameter, $n = 57$ (PBS) vs. $n = 96$ (PSC-EPs). *t*-test. * $P < 0.05$; ** $P < 0.01$.

GFP: green fluorescent protein; PBS: phosphate-buffered saline; PSC-EPs: PSC-derived cells with endothelial potential.

placenta and decreased fetal resorption in the DBA/2-mated CBA/J female mice. The three-dimensional reconstruction of tiling Z-stack images of decidua uncovered massive fetomaternal neovascularization induced by the injection. Remarkably, the injected PSC-EPs seemed to

directly form the spiral arteries, suggesting their ability to migrate, colonize, and establish the functional neovasculation in the decidua, which, in turn, increased blood supply to the placenta. However, our decidua reconstruction analyses have only provided a rough insight into the

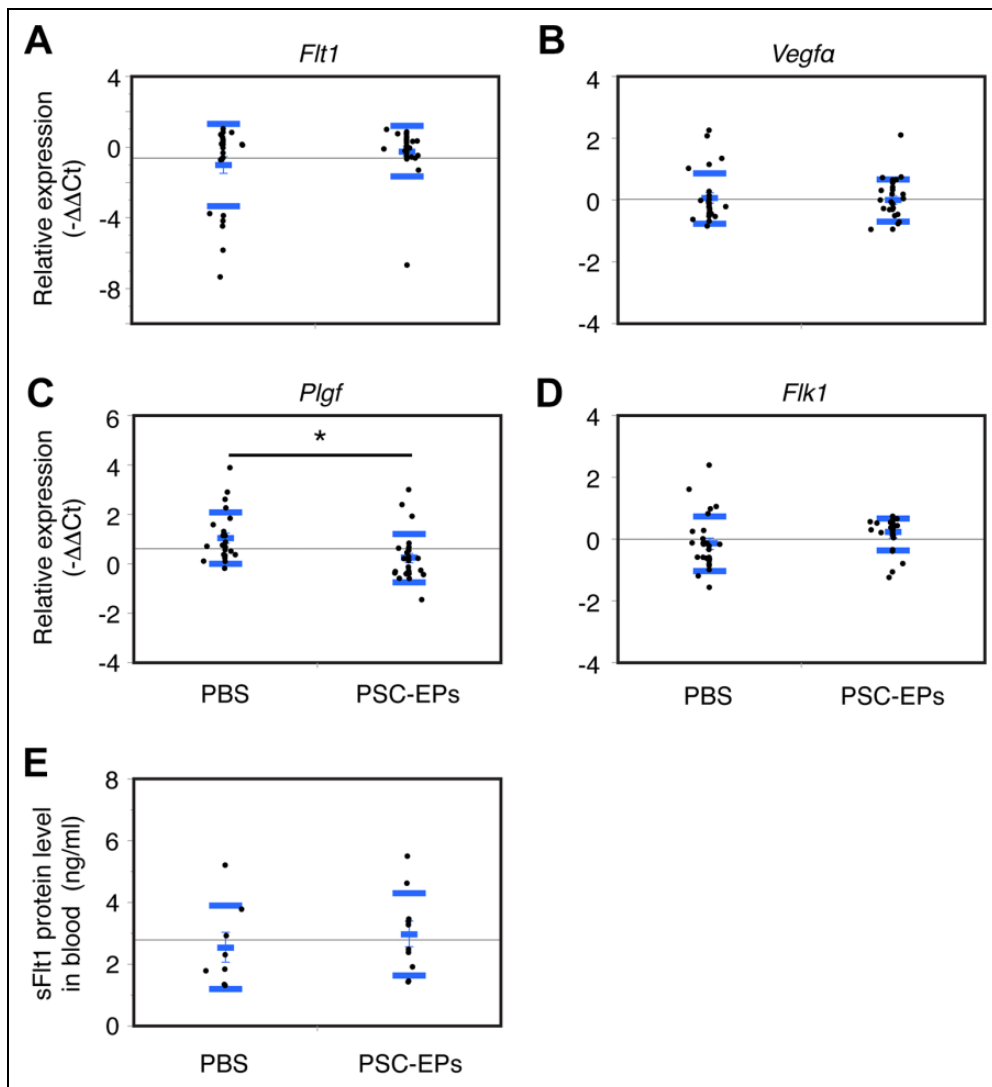


Figure 6. PSC-EP injection does not substantially affect the angiogenic factor balance in DBA/2-mated CBA/J females. (A-D) mRNA expression of the indicated genes in the placenta. RNA was extracted from a placenta of a PBS- or a PSC-EP-injected female mouse. Reverse transcription and quantitative polymerase chain reaction was performed using the extracted RNA. The probes used are indicated. The Ct values obtained with the indicated probes were normalized by those with *Gapdh* (Δ Ct) and then normalized with Δ Cts from the PBS-injected samples ($\Delta\Delta$ Cts). The negative values of the $\Delta\Delta$ Cts are shown in the graph. Mean (short blue bar) \pm SD (long blue bars). In (A, B, and D), $n = 26$ for each group. In (C), $n = 23$ (PBS) vs. $n = 26$ (PSC-EPs). t -test. * $P < 0.05$. (E) Expression of sFlt1 protein in the blood. Blood was collected from a pregnant female mouse, and sFlt1 levels in the blood were quantified by enzyme-linked immunosorbent assay. Mean (short blue bar) \pm SD (long blue bars). $n = 8$ (PBS) vs. $n = 10$ (PSC-EPs). PBS: phosphate-buffered saline; PSC-EPs: PSC-derived cells with endothelial potential.

injected cell contribution to spiral artery formation. Therefore, further investigations, with microscopic and flow cytometric analyses of deciduae as recently reported³¹, are required to answer how and what degree PSC-EPs contribute to the blood vessel formation.

Our results here suggest that IV injection of cells with endothelial potential may effectively treat certain types of human miscarriage. Although we generated and used the ESCs, instead of iPSCs, as PSCs in this study, many studies confirmed

that high-quality ESCs and high-quality iPSCs do not differ in their functionality (e.g., Ref. ³²). Furthermore, unlike other sources (e.g., BM), PSCs could readily provide sufficient numbers of cells to treat pregnant women suffering from recurrent miscarriage. Therefore, we believe our protocol with human iPSCs could become the foundation of a promising treatment for recurrent miscarriage in clinical practice.

Cells on day 4 of the endothelial cell differentiation culture were intravenously injected into pregnant mice. Almost

all the day 4 differentiated cells weakly incorporated Ac-LDLs. Additionally, they efficiently formed vascular-like structures within 24 h under a particular condition *in vitro* despite the low abundance of CD31+ cells. These results suggest that majority of the cells in the differentiation culture may be at a very early endothelial stage but have substantial endothelial potential.

However, the day 4 cultures also contained undifferentiated ESCs, as judged by expression of pluripotent markers, and may have other cell types, but not hematopoietic cells, in mesoderm lineages. Therefore, identification and purification of the cell population that reduces the fetal resorption rate upon IV injection are the next steps toward the clinical use of this treatment. Alternatively, removing undifferentiated ESCs, which may form teratomas, from the culture before transplantation is another way to realize this treatment in clinical practice while maintaining the effectiveness of the treatment. A long-term checkup of female mice and their newborn pups after PSC-EP injection is also required to evaluate any adverse effects of the treatment before considering a clinical trial.

The mouse model used in this study exhibits several features of human miscarriage and preeclampsia. In preeclampsia in humans, based on the “two-stage disorder” theory^{30,33}, failure of spiral artery remodeling (stage 1) subsequently causes several adverse events^{30,34}, such as placental hypoxia/ischemia and angiogenic factor imbalance^{35,36}, and they eventually lead to the disease outcomes (stage 2)^{30,33}. Perhaps the worst episode among possible disease outcomes may be a miscarriage³⁷, and it happens before 20 weeks of pregnancy. In the other milder episodes, embryos could survive beyond 20 weeks, and symptoms of preeclampsia may be manifested after 20 weeks. However, different from humans, since mice exhibit multiple pregnancies, the pregnancy continues even if some of the embryos die, and both miscarriage and preeclampsia-like phenotypes may appear in the same mouse.

Indeed, the insufficient blood supply to the placenta caused by an impairment of spiral artery remodeling results in a fetal loss in the mouse models^{14,15}. In our study, about 30% of the placentae analyzed exhibited hypoperfusion at day 10.5. This hypoperfusion might occur by abnormally immunologically activated NK cells in the decidua, as was observed in the other model mouse¹⁴. The abnormally activated NK cells kill the TGCs that induce spiral artery remodeling. Therefore, it is striking that the PSC-EP injection increased the number, diameter, and density of spiral arteries in the decidua. These increases in fetomaternal neovascularization may be one reason for the amelioration of the fetal loss by increasing blood supply to fetus in the DBA/2-mated CBA/J females. The other possibility is that the cells injected may affect immune responses to the fetus in the mother that is the leading cause of fetal loss. The aberrant immune responses directly damage the fetus by activating the complement-coagulation system^{6,9} or kill TGCs, leading to the impairment of spiral artery remodeling as described

above. In any case, whether the PSC-EP injection affects the immune reactions, NK cells, and TGCs warrants further investigation.

Before our IV protocol here, some treatments for miscarriage and preeclampsia had been proposed using the same mouse model. The mice were treated with statins⁹, thrombomodulin¹⁸, or the complement C3 inhibitor¹¹. These treatments reduced fetal resorption rates and the expression levels of sFlt1, a negative regulator of angiogenesis, by counteracting the abnormally activated complement-coagulation system^{6,9}. The reduced expression of sFlt1 in the placenta and serum may be one of the main factors that ameliorate the preeclampsia phenotypes, including fetal growth restriction. Indeed, the treatment with pravastatin or thrombomodulin enhances fetal growth in the models^{9,18}. However, sFlt1 may not be involved in the fetal resorption because sFlt1 transgenic mice models do not exhibit fetal loss^{16,17}.

In stark contrast to those, our protocol did not significantly alter sFlt1 levels at day 14.5. Consistently, the PSC-EP injection did not enhance fetal growth by day 18.5, although it reduced the resorption even at day 18.5 as same as day 14.5 (Supplemental Fig. 2D, E). Since statins and thrombomodulin were injected several times into mice, in contrast to the one-time injection of PSC-EPs in this study, modifying the PSC-EP injection protocol may prevent the fetal growth restriction and other preeclampsia phenotypes in this model. Alternatively, the observations suggest that our protocol and the other proposed treatments differ in how they prevent fetal loss. Therefore, our protocol may have synergistic therapeutic effects on miscarriage and preeclampsia, in conjunction with the other treatments. Indeed, BM-derived EPCs showed a synergistic effect with thrombomodulin to treat hindlimb ischemia mice³⁸. The synergistic therapeutic effects deserve further investigation.

Since the first mouse ESCs were reported in 1981^{39,40}, they have been used in several fields, including mouse genetic engineering, and become indispensable materials for post-genome research and regenerative medicine research^{41–43}. Development of the LIF+2i culture condition²⁵ enabled us to derive several ESC lines from various mouse strains, such as NOD and DBA⁴⁴. Indeed, ESC lines were also generated from CBA/CA under a similar condition⁴⁴. However, as far as we know, CBA/J-derived ESC lines have never been reported. Although both CBA/CA and CBA/J originated from CBA mouse, their differences are too significant to be histocompatible⁴⁵, prompting us to derive ESCs from CBA/J-mated female CBA/J. Because CBA/J mice specifically exhibit several disease phenotypes, including miscarriage and renal tubulointerstitial lesions⁴⁶, the mouse ESCs we established may contribute to the several fields in which the disease phenotypes are involved.

Previous reports, including ours¹⁹, showed that the transplantation of cord blood-, PB-, or BM-derived EPCs promotes neovascularization that ameliorates the disease phenotypes, including hindlimb ischemia, in several animal models^{47–49}. Additionally, some clinical trials with

PB-derived EPCs or BM mononuclear cells containing EPCs showed the effectiveness of the therapeutic angiogenesis for limb ischemia^{50,51}. However, additional hurdles must be crossed before clinical practice using therapeutic angiogenesis. First, only a limited number of EPCs can be collected from a patient. Second, the functionality of the collected EPCs is unclear, and they may exhibit the treatment effects by producing soluble humoral factors that modulate angiogenesis or by modulating immune reactions in donors.

Our protocol can produce an unlimited number of cells, as many as we need for transplantation. Also, we showed that the intravenously injected PSC-EPs seem to form spiral arteries robustly without affecting the humoral factor expressions, suggesting their outstanding ability in neovascularization. However, in this study, we did not examine if the injected PSC-EPs impact the mothers' immune responses, which is strongly involved in the fetal loss in this mouse model as described. Thus, we cannot exclude the possibility of immunological effects of our protocol. Furthermore, the expressions of the secreted factors, including sFlt1, vary depending on gestation stages analyzed (e.g., Ref. ⁶). Therefore, in addition to the direct effects of the PSC-EPs on neovascularization, their effects on immunomodulation and the secreted factor expressions warrant further investigation to apply them for clinical applications.

The differentiation protocol we used was developed to differentiate human PSCs to endothelial cells²¹. It took only 4 days after starting the differentiation to prepare cells for the injection. Thus, one can easily apply the same protocol for preparing human PSC-EPs for clinical use. Although some discrete subjects described above need to be addressed, we envision using a treatment based on our protocol for recurrent miscarriage and preeclampsia in clinical practice in the near future.

Acknowledgments

We thank the Asahi lab for the support and useful discussions. We also would like to thank NPO Biotechnology Research and Development for the chimeric mouse generation.

Authors Contribution

Conceptualization, KT, MO, and MA; Methodology, AD, HM, KK, and KT; Mouse ESC derivation, YK, AD, and KT; Intravenous injection, HM; Formal analysis, AD and KT; Investigation, AD and KT; Resources, KT and MA; Writing—original draft, AD and KT; Writing—revision and editing, AD, KT, and MA; Visualization, AD and KT; Supervision, KT, MO, and MA; Project administration, KT; Funding acquisition, KK, KT, and MA.

Ethical Approval

Ethical approval is not applicable to this article.

Statement of Human and Animal Rights

All animal procedures were performed in compliance with the guidelines of the Osaka Medical College Animal Care and Use Committee (No. 2019-084). This article does not contain any studies with humans.

Statement of Informed Consent

There are no human subjects in this article, and informed consent is not applicable.

Declaration of Conflicting Interests

The author(s) declared no potential conflicts of interest with respect to the research, authorship, and/or publication of this article.

Funding

The author(s) disclosed receipt of the following financial support for the research, authorship, and/or publication of this article: This work was supported in part by a JSPS KAKENHI grant (to KK, number 16K11119), the Suzuki Memorial Foundation (to KT), and the OMC Internal Research Grant (to MA).

ORCID iDs

Atsushi Daimon  <https://orcid.org/0000-0001-8196-4597>
Kiichiro Tomoda  <https://orcid.org/0000-0002-2024-311X>

Supplemental Material

Supplemental material for this article is available online.

References

1. Practice Committee of the American Society for Reproductive M. Evaluation and treatment of recurrent pregnancy loss: a committee opinion. *Fertil Steril*. 2012;98(5):1103–1111.
2. Shahine L, Lathi R. Recurrent pregnancy loss: evaluation and treatment. *Obstet Gynecol Clin North Am*. 2015;42(1):117–134.
3. Empson M, Lassere M, Craig J, Scott J. Prevention of recurrent miscarriage for women with antiphospholipid antibody or lupus anticoagulant. *Cochrane Database Syst Rev*. 2005;2005(2):CD002859.
4. Bobe P, Chaouat G, Stanislawski M, Kiger N. Immunogenetic studies of spontaneous abortion in mice. II. Antiabortive effects are independent of systemic regulatory mechanisms. *Cell Immunol*. 1986;98(2):477–485.
5. Clark DA, Chaouat G, Arck PC, Mittrucker HW, Levy GA. Cytokine-dependent abortion in CBA x DBA/2 mice is mediated by the procoagulant fgl2 prothrombinase [correction of prothombinase]. *J Immunol*. 1998;160(2):545–549.
6. Girardi G, Yarilin D, Thurman JM, Holers VM, Salmon JE. Complement activation induces dysregulation of angiogenic factors and causes fetal rejection and growth restriction. *J Exp Med*. 2006;203(9):2165–2175.
7. Clark DA, Chaouat G, Banwatt D, Friebe A, Arck PC. Ecology of danger-dependent cytokine-boosted spontaneous abortion in the CBA x DBA/2 mouse model: II. Fecal LPS levels in colonies with different basal abortion rates. *Am J Reprod Immunol*. 2008;60(6):529–533.
8. Girardi G. Complement inhibition keeps mothers calm and avoids fetal rejection. *Immunol Invest*. 2008;37(5):645–659.
9. Redecha P, van Rooijen N, Torry D, Girardi G. Pravastatin prevents miscarriages in mice: role of tissue factor in placental and fetal injury. *Blood*. 2009;113(17):4101–4109.

10. Ahmed A, Singh J, Khan Y, Seshan SV, Girardi G. A new mouse model to explore therapies for preeclampsia. *PLoS One*. 2010;5(10):e13663.
11. Qing X, Redecha PB, Burmeister MA, Tomlinson S, D'Agati VD, Davission RL, Salmon JE. Targeted inhibition of complement activation prevents features of preeclampsia in mice. *Kidney Int*. 2011;79(3):331–339.
12. Clark DA. The importance of being a regulatory T cell in pregnancy. *J Reprod Immunol*. 2016;116:60–69.
13. Clark DA. The use and misuse of animal analog models of human pregnancy disorders. *J Reprod Immunol*. 2014;103:1–8.
14. Yougbare I, Tai WS, Zdravic D, Oswald BE, Lang S, Zhu G, Leong-Poi H, Qu D, Yu L, Dunk C, Zhang J, et al. Activated NK cells cause placental dysfunction and miscarriages in fetal alloimmune thrombocytopenia. *Nat Commun*. 2017;8(1):224.
15. Hu D, Cross JC. Ablation of Tpbpa-positive trophoblast precursors leads to defects in maternal spiral artery remodeling in the mouse placenta. *Dev Biol*. 2011;358(1):231–239.
16. Burke SD, Zsengeller ZK, Khankin EV, Lo AS, Rajakumar A, DuPont JJ, McCurley A, Moss ME, Zhang D, Clark CD, Wang A, et al. Soluble fms-like tyrosine kinase 1 promotes angiotensin II sensitivity in preeclampsia. *J Clin Invest*. 2016;126(7):2561–2574.
17. Kumasawa K, Ikawa M, Kidoya H, Hasuwa H, Saito-Fujita T, Morioka Y, Takakura N, Kimura T, Okabe M. Pravastatin induces placental growth factor (PGF) and ameliorates preeclampsia in a mouse model. *Proc Natl Acad Sci U S A*. 2011;108(4):1451–1455.
18. Sano T, Terai Y, Daimon A, Nunode M, Nagayasu Y, Okamoto A, Fujita D, Hayashi M, Ohmichi M. Recombinant human soluble thrombomodulin as an anticoagulation therapy improves recurrent miscarriage and fetal growth restriction due to placental insufficiency - The leading cause of preeclampsia. *Placenta*. 2018;65:1–6.
19. Kanki K, Ii M, Terai Y, Ohmichi M, Asahi M. Bone marrow-derived endothelial progenitor cells reduce recurrent miscarriage in gestation. *Cell Transplant*. 2016;25(12):2187–2197.
20. Czechanski A, Byers C, Greenstein I, Schrode N, Donahue LR, Hadjantonakis AK, Reinholdt LG. Derivation and characterization of mouse embryonic stem cells from permissive and nonpermissive strains. *Nat Protoc*. 2014;9(3):559–574.
21. Lian X, Bao X, Al-Ahmad A, Liu J, Wu Y, Dong W, Dunn KK, Shusta EV, Palecek SP. Efficient differentiation of human pluripotent stem cells to endothelial progenitors via small-molecule activation of WNT signaling. *Stem Cell Reports*. 2014;3(5):804–816.
22. Hayashi K, Ohta H, Kurimoto K, Aramaki S, Saitou M. Reconstitution of the mouse germ cell specification pathway in culture by pluripotent stem cells. *Cell*. 2011;146(4):519–532.
23. Tainaka K, Kubota SI, Suyama TQ, Susaki EA, Perrin D, Ukai-Tadenuma M, Ukai H, Ueda HR. Whole-body imaging with single-cell resolution by tissue decolorization. *Cell*. 2014;159(4):911–924.
24. Morizane A, Doi D, Kikuchi T, Okita K, Hotta A, Kawasaki T, Hayashi T, Onoe H, Shiina T, Yamanaka S, Takahashi J. Direct comparison of autologous and allogeneic transplantation of iPSC-derived neural cells in the brain of a non-human primate. *Stem Cell Reports*. 2013;1(4):283–292.
25. Ying QL, Wray J, Nichols J, Battle-Morera L, Doble B, Woodgett J, Cohen P, Smith A. The ground state of embryonic stem cell self-renewal. *Nature*. 2008;453(7194):519–523.
26. Theodoris CV, Li M, White MP, Liu L, He D, Pollard KS, Bruneau BG, Srivastava D. Human disease modeling reveals integrated transcriptional and epigenetic mechanisms of NOTCH1 haploinsufficiency. *Cell*. 2015;160(6):1072–1086.
27. Autengruber A, Gereke M, Hansen G, Hennig C, Bruder D. Impact of enzymatic tissue disintegration on the level of surface molecule expression and immune cell function. *Eur J Microbiol Immunol*. 2012;2(2):112–120.
28. Adamson SL, Lu Y, Whiteley KJ, Holmyard D, Hemberger M, Pfarrer C, Cross JC. Interactions between trophoblast cells and the maternal and fetal circulation in the mouse placenta. *Dev Biol*. 2002;250(2):358–373.
29. Li C, Piran S, Chen P, Lang S, Zarpellon A, Jin JW, Zhu G, Rehemana A, van der Wal DE, Simpson EK, Ni R, et al. The maternal immune response to fetal platelet GPIIb/IIIa causes frequent miscarriage in mice that can be prevented by intravenous IgG and anti-FcRn therapies. *J Clin Invest*. 2011;121(11):4537–4547.
30. Wang A, Rana S, Karumanchi SA. Preeclampsia: the role of angiogenic factors in its pathogenesis. *Physiology (Bethesda)*. 2009;24:147–158.
31. Tal R, Dong D, Shaikh S, Mamillapalli R, Taylor HS. Bone-marrow-derived endothelial progenitor cells contribute to vasculogenesis of pregnant mouse uterus. *Biol Reprod*. 2019;100(5):1228–1237.
32. Zhao X-y, Li W, Lv Z, Liu L, Tong M, Hai T, Hao J, Guo C-l, Ma Q-w, Wang L, Zeng F, et al. iPSC cells produce viable mice through tetraploid complementation. *Nature* 2009;461(7260):86–90.
33. Roberts JM, Hubel CA. The two stage model of preeclampsia: variations on the theme. *Placenta*. 2009;30(suppl A):S32–37.
34. Pijnenborg R, Anthony J, Davey DA, Rees A, Tiltman A, Vercruyssen L, van Assche A. Placental bed spiral arteries in the hypertensive disorders of pregnancy. *Br J Obstet Gynaecol*. 1991;98(7):648–655.
35. Karumanchi SA, Bdolah Y. Hypoxia and sFlt-1 in preeclampsia: the “chicken-and-egg” question. *Endocrinology*. 2004;145(11):4835–4837.
36. Nagamatsu T, Fujii T, Kusumi M, Zou L, Yamashita T, Osuga Y, Momoeda M, Kozuma S, Taketani Y. Cytotrophoblasts up-regulate soluble fms-like tyrosine kinase-1 expression under reduced oxygen: an implication for the placental vascular development and the pathophysiology of preeclampsia. *Endocrinology*. 2004;145(11):4838–4845.
37. Jivraj S, Anstie B, Cheong YC, Fairlie FM, Laird SM, Li TC. Obstetric and neonatal outcome in women with a history of recurrent miscarriage: a cohort study. *Hum Reprod*. 2001;16(1):102–106.
38. Li JY, Su CH, Wu YJ, Tien TY, Hsieh CL, Chen CH, Tseng YM, Shi GY, Wu HL, Tsai CH, Lin FY, et al. Therapeutic

- angiogenesis of human early endothelial progenitor cells is enhanced by thrombomodulin. *Arterioscler Thromb Vasc Biol.* 2011;31(11):2518–2525.
39. Evans MJ, Kaufman MH. Establishment in culture of pluripotential cells from mouse embryos. *Nature.* 1981;292(5819):154–156.
 40. Martin GR. Isolation of a pluripotent cell line from early mouse embryos cultured in medium conditioned by teratocarcinoma stem cells. *Proc Natl Acad Sci U S A.* 1981;78(12):7634–7638.
 41. Palacios R, Golunski E, Samaridis J. *In vitro* generation of hematopoietic stem cells from an embryonic stem cell line. *Proc Natl Acad Sci U S A.* 1995;92(16):7530–7534.
 42. Klug MG, Soonpaa MH, Koh GY, Field LJ. Genetically selected cardiomyocytes from differentiating embryonic stem cells form stable intracardiac grafts. *J Clin Invest.* 1996;98(1):216–224.
 43. Brustle O, Jones KN, Learish RD, Karram K, Choudhary K, Wiestler OD, Duncan ID, McKay RD. Embryonic stem cell-derived glial precursors: a source of myelinating transplants. *Science* 1999;285(5428):754–756.
 44. Buehr M, Smith A. Genesis of embryonic stem cells. *Philos Trans R Soc Lond B Biol Sci.* 2003;358(1436):1397–1402; discussion 1402.
 45. Green MC, Kaufer KA. A test for histocompatibility between sublines of the CBA strain of mice. *Transplantation.* 1965;3(6):766–768.
 46. Rudofsky UH. Renal tubulointerstitial lesions in CBA/J mice. *Am J Pathol.* 1978;92(2):333–348.
 47. Murohara T, Ikeda H, Duan J, Shintani S, Sasaki K, Eguchi H, Onitsuka I, Matsui K, Imaizumi T. Transplanted cord blood-derived endothelial precursor cells augment postnatal neovascularization. *J Clin Invest.* 2000;105(11):1527–1536.
 48. Kalka C, Masuda H, Takahashi T, Kalka-Moll WM, Silver M, Kearney M, Li T, Isner JM, Asahara T. Transplantation of ex vivo expanded endothelial progenitor cells for therapeutic neovascularization. *Proc Natl Acad Sci U S A.* 2000;97(7):3422–3427.
 49. Shintani S, Murohara T, Ikeda H, Ueno T, Sasaki K, Duan J, Imaizumi T. Augmentation of postnatal neovascularization with autologous bone marrow transplantation. *Circulation.* 2001;103(6):897–903.
 50. Tateishi-Yuyama E, Matsubara H, Murohara T, Ikeda U, Shintani S, Masaki H, Amano K, Kishimoto Y, Yoshimoto K, Akashi H, Shimada K, et al. Therapeutic angiogenesis for patients with limb ischaemia by autologous transplantation of bone-marrow cells: a pilot study and a randomised controlled trial. *Lancet.* 2002;360(9331):427–435.
 51. Liotta F, Annunziato F, Castellani S, Boddi M, Alterini B, Castellini G, Mazzanti B, Cosmi L, Acquafresca M, Bartalesi F, Dilaghi B, et al. Therapeutic efficacy of autologous non-mobilized enriched circulating endothelial progenitors in patients with critical limb ischemia- the SCelta trial. *Circ J.* 2018;82(6):1688–1698.